

Single and combined neurotoxic, cytotoxic and genotoxic effects of 5GHz MIMO waves and computed tomography irradiation in male Wistar rats

Adejoke Olukayode Obajuluwa^{id}^a, James C. Lech^{id}^b, Danlami Amina^a, Chidiogo Chukwunweike Onwuka^{id}^c, Rahman Ayodele Bolarinwa^{id}^d, Tiwalola Madoc Obajuluwa^{id}^e, Adedamola Adediran Fafure^{id}^f, Tjaart P.J. Krüger^{id}^g, Olakunle Bamikole Afolabi^h, Abel Anish^c, Olusegun Emoruwaⁱ and Malcolm Baker^j

^aDepartment of Biological Sciences (Biotechnology Unit), Afe Babalola University, Ado Ekiti, Nigeria; ^bDepartment of Radiology and Nuclear Medicine, Academic Medical Centre, University of Amsterdam (UMC), Amsterdam, The Netherlands; ^cRadiology Unit, Afe Babalola University MultiSystem Hospital, Ado Ekiti, Nigeria; ^dIle Ife, Obafemi Awolowo University Teaching Hospital, Ado Ekiti, Nigeria; ^eMedia and Communications Department, Afe Babalola University, Ado Ekiti; ^fDepartment of Anatomy, Afe Babalola University, Ado Ekiti, Nigeria; ^gDepartment of Physics, University of Pretoria, South Africa; ^hDepartment of Biochemistry, Afe Babalola University, Ado Ekiti, Nigeria; ⁱICT Unit, Computer Networking, Afe Babalola University, Ado Ekiti; ^jDepartment of Neurology, Military Hospital, Pretoria, South Africa

ABSTRACT

A significant public concern is how technologies that emit electromagnetic waves interact and affect the biota because they are linked to the dysregulation of genes involved in neurotransmission, oxidative stress, and normal cellular function. Standard methods have been used to study how the combination of electromagnetic waves from 5 GHz radio and computed tomography (CT) irradiation affects whole blood parameters, neurobehavioural profiles, genomic DNA, and *p53* gene expression in *Wistar* rats grouped into five, namely, I-Negative control, II-sham, III-5 GHz only, IV-5 GHz + CT, V-CT. The 5 GHz router was connected to the internet using an ethernet cable and the specific absorbance rate (SAR) was measured as 0.54W/kg and 24 V/0.5A power density, while CT parameters were set at 140 K.v, 300 mA, 5.3 cv at a 1.0-s speed for 60 s. Genomic DNA was isolated from rats' cerebral cortex, while target gene and internal control primers (*GAPDH*) were synthesized for tumor suppressor (*p53*) gene expression and electrophoresed on a 1.2% agarose gel. We found that CT irradiation had gross effects on platelets, white blood cell counts, memory, hepatic and testicular histoarchitectures compared to the 5 GHz-only group. However, there was a loss of *p53* (exons 5–7) gene bands in electrophoresed data with increased micronucleated polychromatic erythrocyte count in the 5 GHz group. Regardless of the interferential interaction in the combination group, the deleterious effects of non-ionizing and ionizing irradiation in the single and combined exposure groups predict functional abnormalities and dysregulated cellular processes from high electromagnetic fields exposure in biological systems.

ARTICLE HISTORY

Received 2 August 2023
Revised 9 October 2023
Accepted 07 November 2023

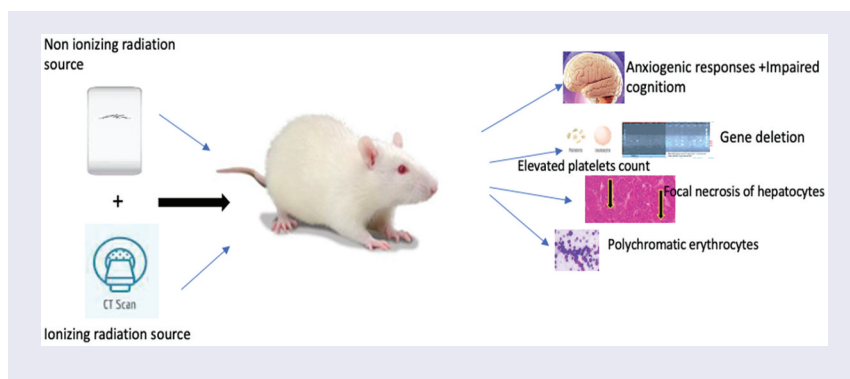
KEYWORDS

Electromagnetic fields; blood platelets; memory; cognition; gene expression; photon

CONTACT Adejoke Olukayode Obajuluwa ibitayoao@abuad.edu.ng Department of Biological Sciences (Biotechnology Unit), Afe Babalola University, Ado Ekiti, Ekiti State, Nigeria

© 2023 The Author(s). Published by Informa UK Limited, trading as Taylor & Francis Group.

This is an Open Access article distributed under the terms of the Creative Commons Attribution-NonCommercial License (<http://creativecommons.org/licenses/by-nc/4.0/>), which permits unrestricted non-commercial use, distribution, and reproduction in any medium, provided the original work is properly cited. The terms on which this article has been published allow the posting of the Accepted Manuscript in a repository by the author(s) or with their consent.



Introduction

In recent years, there has been a significant global surge in the utilization of non-ionizing and ionizing radiofrequency (RF) electromagnetic fields (EMFs) for a diverse array of applications in daily life, including communication, diagnostics, therapeutics, and various other areas [1]. These sources of RF emissions encompass established wireless network systems, the contentious 5 G wireless network, ultraviolet and infrared radiation, as well as X-rays used in computed tomography scans. These technologies are rapidly evolving and hold paramount importance in the sustainability and advancement of societal structures and systems on a global scale. Sensitivity and intolerance to non-native EMF emissions, which manifest in a manner contingent upon the level of exposure, have been associated with a range of symptoms such as tinnitus, headaches, dizziness, irregular heartbeats, memory issues, and sleep disturbances. This condition is commonly referred to as 'Electromagnetic Hypersensitive Syndrome (EHS)' or 'Electromagnetic Field Intolerance Syndrome (EMFIS)' [2,3]. Moreover, extended exposure to EMF radiation has been linked to various physiological alterations, impacting both the central nervous system and the male reproductive system [4–6]. It has also been associated with adverse effects on stress hormones, sperm cells [7,8], as well as oxidative stress and the generation of reactive oxygen species [9] in animal studies. *In-vivo* studies have provided evidence of

impairment of motor coordination, locomotor behavior and increased genetic material damage, and disruption of cholinergic pathway genes, resulting from prolonged exposure to EMF waves [10–12]. Furthermore, some studies have suggested a potential connection between non-native EMF wave exposure and genes governing cell proliferation, potentially increasing the risk of cancer and other health issues [13,14]. The tumor suppressor protein p53 plays a pivotal role in regulating cellular responses to radiation. Accumulation of p53 within cells is triggered by DNA damage, and it serves as a multifunctional nuclear transcription factor that regulates processes such as cell maturation, proliferation, metabolism, immune response, and more. The induction of p53 in response to mutagenic or genotoxic factors, including radiation, promotes protein translation, which is implicated in the pathogenesis of various types of cancer. Additionally, mutant p53 has been implicated as an inhibitory factor for autophagy and programmed cell death in the cytoplasm [15]. Mitochondrial health is maintained through the process of autophagy, which removes damaged and permeabilized mitochondria from cells [16,17]. However, in the presence of mutagenic factors such as radiation, this crucial process may become dysregulated. Consequently, there has been a heightened focus on research efforts in recent years to comprehensively investigate the effects of increased exposure to both ionizing and

non-ionizing radiation. Hence, the endeavors to contribute to the development of evidence-based solutions in the field of EMF exposure and their potential impact on human health and biology. Therefore, the present study investigated the physiological and genetic consequences of single and combined ionizing and non-ionizing radiation exposure on complete blood count, memory, cognition, *p53* exons 5–7 bands detection, histopathological indices and micronucleus formation in rats.

Materials and methods

Animals and study design

Male virgin *Wistar* rats (50–60 days old) weighing 120 ± 30 g were supplied by the animal breeding unit at the College of Medicine, Afe Babalola University. All rats were kept in standard laboratory conditions with a 12:12 photon periodism light–dark regimen and tap water and food given *ad libitum*. Animal groupings [$n=6$] were i) negative control, ii) Sham irradiated, iii) 5-GHz irradiated, iv) 5 GHz + CT irradiated, and v) CT only irradiated.

Non-native electromagnetic field exposure

Radiofrequency (RF) generator setup

An off-the-shelf commercially available wireless router [M5 airMax 16dBi CPE,25 V:0.5A PoE] was used with a multiple-input multiple-output (MIMO) transmission protocol set at 5 GHz frequency band. The irradiated electric field density was set at 100 cm measured a median of 11 V/m. The router was connected to the internet using an ethernet cable, no Wi-Fi repeater was used. The specific absorbance rate (SAR) was measured as 0.54W/kg.

Rats RF irradiation setup

Rats in groups III and IV were kept 100 cm away from the router to allow for a whole-body RF-far-field irradiation zone from 9 am to 5 pm. In a separate room, two groups of negative control

rats were placed in UV-blocking plexiglass cages, while rats in the sham group were placed in the same housing condition as rats in 5 GHz excluding irradiation, in another room.

Rats CT irradiation setup

On day 14 of exposure, fractionated computed tomography (CT) scans at a dose rate of 196 mGy and 73.68 mGy for 60 s were given at 100 cm distance from the beam exit to rats in groups IV and V at scanning parameters: 140 K.v, 300 mA, 5.3 cv at a 1.0-s speed for 60 s while group II was CT-sham irradiated. The field size of the LINAC accelerator was 40×40 cm². This procedure was carried out at the Radiology Unit, ABUAD Multisystem Hospital.

Y-maze and novel object recognition (NOR) tests

The spontaneous alternation test (Y-maze) was used to assess spatial working memory performance by measuring experimental rats' tendency to alternate arm entries, locomotor activity through arm entry frequency and number of triads at 14 days post 5 GHz and 24-h CT irradiation exposure. The NOR tests were also carried out as described by Lueptow [18].

Haematology estimation

Animals were sacrificed upon completion of behavioral assays by anesthetic overdose, and blood was collected via cardiac puncture in labeled sterile EDTA vacutainers. An automated hematology analyzer (Mindray, BC 6000) was used for whole blood count bioassays (red blood cell, white blood cell, lymphocyte, hemoglobin, red blood cell, and mean corpuscular volume, etc.).

DNA extraction and fragmentation analyses

Genomic DNA was isolated from rats' brain cortex using ZymoResearch tissue DNA extraction

kit. Purity assessment and nucleic acid quantification were carried out immediately after extraction with 1 µl of sample in Nanodrop 2.0. Two microliters of isolated DNA were loaded with 1kb DNA ladder and dye in 1.2% agarose gel stained with ethidium bromide and ran at 100 V/cm for 1 hr at room temperature. The bands were captured with a UV transilluminator. Isolated DNA was stored in aliquots at -20°C until further use for further analyses.

Polymerase chain reaction and p53 agarose gel electrophoresis profiles in rats' brain tissue

The PCR amplifications of *p53* exons 5–7 were performed at 95°C for 5 min (denaturation), annealing for 1 min, and then extension at 72°C for 1 min for 40 cycles, while each included denaturation at 95°C for 1 min. The amplicons were loaded into 1.2% agarose gel and run at 75 V for 1 hr at room temperature. Gel visualization was carried out in a UV transilluminator, while thermal cycling for *p53* exons and *GAPDH* (internal control) were run separately based on different annealing temperatures using sequenced primers in Table 1.

Histopathological analysis

Testes and livers of rats stored in 10% formal saline were processed using established laboratory protocols. Processed tissues were sectioned ($5\ \mu\text{m}$ thick) on slides and stained using the Hematoxylin and Eosin (H&E) technique.

Table 1. Sequenced primers for *p53* gene expression.

Gene	Primer
<i>P₅₃</i> exon 5	F: GACCTTTGATTCTTTCTCCTCTCC R: GGGAGACCCCTGGACAACCAG
<i>P₅₃</i> exon 6–7	F: CTGGTTGTCCAGGGTTCTCC R: CCCAACCTGGCACACAGCTT
<i>GAPDH</i>	F: ACCACAGTCCATGCCATCAC R: TCCACCACCTGTTGCTGTA

Micronucleus count

Bone marrow cells were excised from the femurs of rats using hypodermic needles containing 0.05 mL of fetal calf serum. Smears on microscopic slides were stained with May-Grunwald (5 min) and Giemsa (10 min) accordingly. Slides were scored with an Olympus X microscope.

Histopathological analysis

Testes and livers of rats stored in 10% formal saline were processed using established laboratory protocols. Processed tissues were sectioned ($5\ \mu\text{m}$ thick) on slides and stained using the Hematoxylin and Eosin (H&E) technique.

Micronucleus count

Bone marrow cells were excised from the femurs of rats using hypodermic needles containing 0.05 mL of fetal calf serum. Smears on microscopic slides were stained with May-Grunwald (5 min) and Giemsa (10 min) accordingly. Slides were scored with an Olympus X microscope.

Results

Memory and cognition indices in irradiated rats

Percentage alternation and number of entries were significantly reduced in the single (5 GHz) and combined (5 GHz + CT) groups in the Y-maze apparatus ($<60\%$, $p < 0.05$) (Figure 1), lowest number of entries was recorded in the CT exposed rats ($p < 0.01$).

As seen in Figure 2, NOR was significantly higher in negative control and sham-irradiated rats ($p < 0.001$). Gross NOR impairments were observed in the CT-irradiated rats ($p < 0.001$) compared to the single 5 GHz and combined (5 GHz + CT) groups.

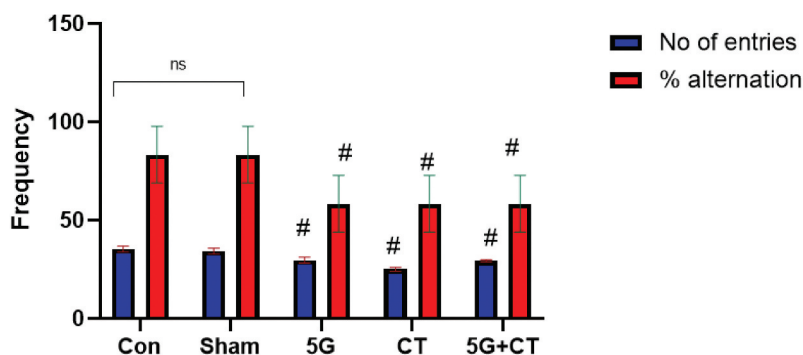


Figure 1. Single and combined effects of 5GHz and CT irradiation on cognition in rats. (Key: # = low)

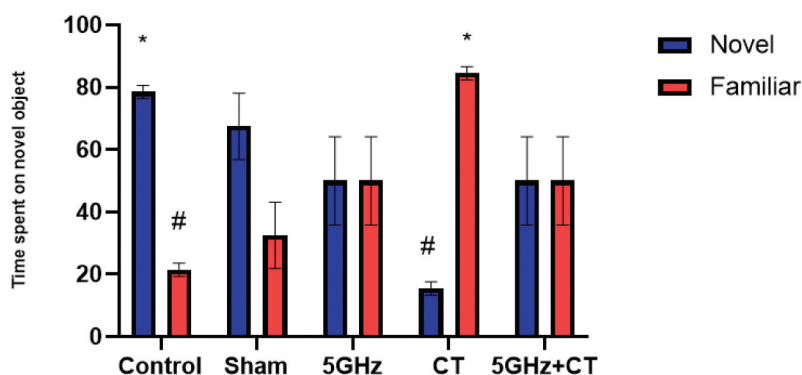


Figure 2. Single and combined effects of 5 GHz and CT nor indicates in rats. (Key: * = high, # = low)

Effects of 5 GHz and/or CT radiation on rats' haematology

Figure 3 shows abnormally high platelets count in the CT group ($p < 0.0001$) and combined 5 GHz + CT rats ($p < 0.01$), while an inverse effect (abnormally low levels) was seen in the 5 GHz group ($p < 0.001$). Granulocyte count was significantly higher in 5 GHz ($p < 0.01$), while lymphocyte count was significantly decreased ($p < 0.05$) in the CT group. Reduced white blood cell counts were observed for rats exposed to 5 GHz, CT, and 5 GHz + CT.

Genomic DNA fragments in irradiated rats

Intact gDNA band sizes were observed in the control, combined radiation group and CT compared to the sham-irradiated group and

degraded DNA bands profiles in the 5 GHz group (Figure 4a). The PCR amplification of exon 5–7 produced 260 bp, 300 bp and 175 bp amplicon sizes, respectively (Figs B&C). A complete loss of *p53* (ex 5–7) bands were seen in the 5 GHz group, while indistinct exon 7 bands were observed in the combined (5 GHz + CT) and CT-only groups.

Degeneration of hepatocytes

Distinct normal arrangement of the hepatocytes (black arrow) is seen in control and sham groups compared to the irradiated groups (Figure 5, $***p < 0.001$). The 5 GHz group reveals vacuolation and moderate degeneration of hepatocytes (black arrow). The CT-irradiated group reveals necrosis and severe degeneration of the hepatocytes

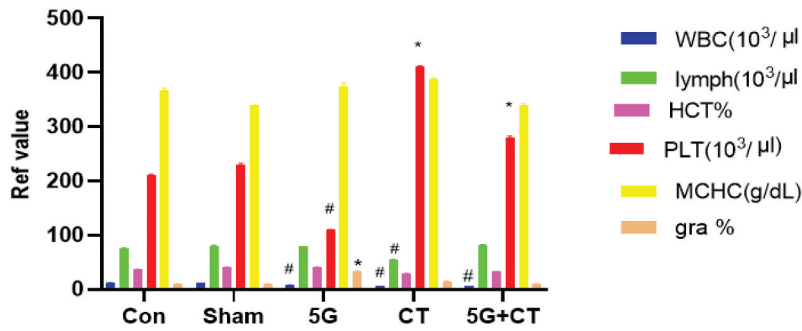


Figure 3. Single and combined effects of 5 GHz and CT-irradiation radiation on rats' blood parameters. GenomicDNA fragments in irradiated rats. (Key: * = high, # = low)

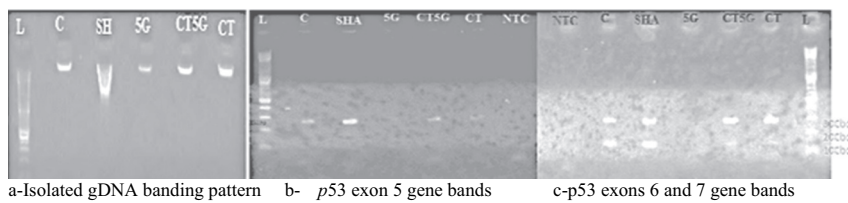


Figure 4. Agarose gel electrophoresis of gDNA (a) and p53 exon 5–7 (b & c) gene expression in rats. Key: L = Ladder (1kb plus size), C = Control, SH = sham, CT = CT irradiated, 5 G = 5 GHz waves exposed, CT5G = combined 5 G and CT exposure, NTC = no template control

(black arrow: degenerated hepatocytes). The 5 GHz + CT group reveals a statistically significant decrease in liver cell count when compared to the 5 GHz group only (***) $p < 0.001$.

Fig. '5'. Liver of rat from I) negative control showing normal histoarchitecture and arrangement of hepatocytes (black arrow) II) sham group showing moderate vacuolation and

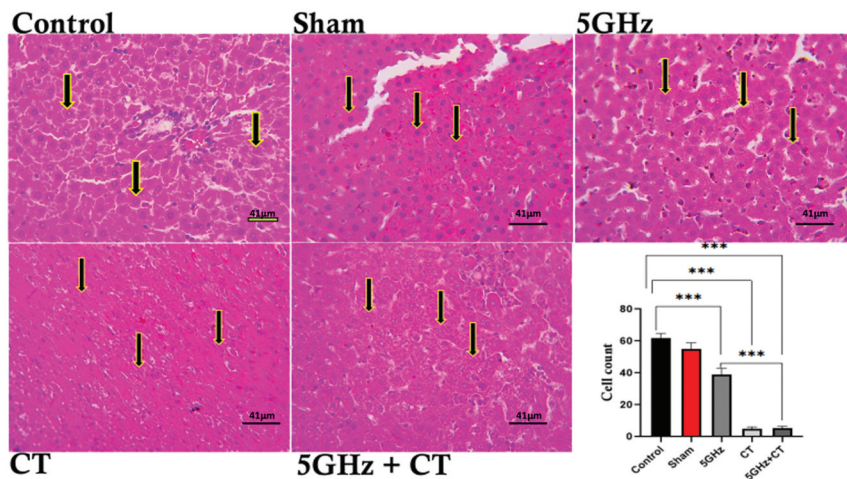


Figure 5. Histological alteration of the liver cells (hepatocytes) following exposure to 5 GHz, CT-irradiation, 5 GHz + CT irradiation. Photomicrographs at 800X magnification (scale bar: 41 μm), using H&E staining.

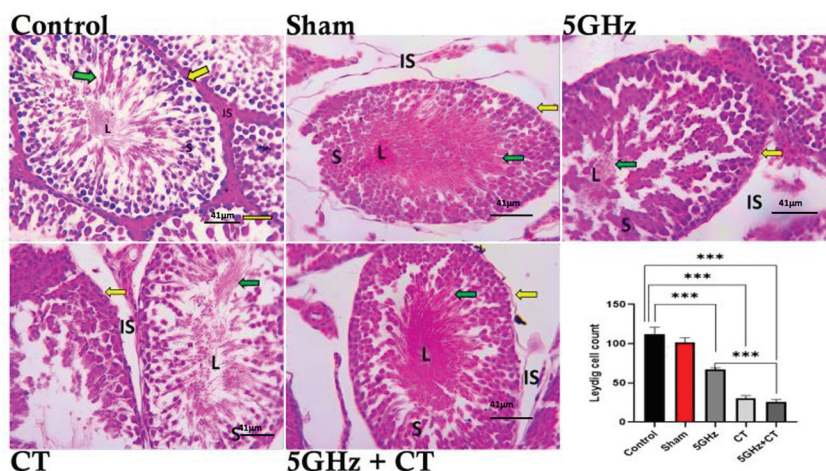


Figure 6. Histological alteration of the testis (seminiferous tubules) following exposure to 5 GHz, CT-irradiation, 5 GHz + CT irradiation. Photomicrographs at 800× magnification (scale bar: 41 μm), using H&E staining.

normal arrangement of hepatocytes III) 5 GHz irradiated group showed moderate degeneration of hepatocytes IV) CT irradiated groups showing indistinct arrangement and necrosis of hepatocytes, while V) 5 GHz + CT irradiated group shows hepatocytes degeneration with a $p < 0.001$ level of statistical significance when compared to other groups (H&E scale bar 41 μm).

Degeneration of seminiferous tubules epithelium (STE) and Leydig cell count

The normal arrangement of STE, clusters of sperm cells at the lumen and a statistically significant increase in Leydig cells ($***p < 0.001$) is seen in control and sham groups. The 5 GHz irradiation group reveals mild degeneration of STE, loss of sperm cells at the lumen, and degeneration of the interstitial cells. The CT-irradiation group revealed severe degeneration of STE, loss of sperm cells at the lumen and a statistically significant reduction of the Leydig cells. The 5 GHz + CT group reveals a moderate loss of STE and a statistical reduction of interstitial cells.

Figure 6 Testis of rat from I) negative control, showing the normal histological structure of

seminiferous tubules with normal spermatogonial cells and complete spermatogenesis with sperm production, II) Sham irradiated group same as in control. III) 5 GHz irradiated group showing mild degeneration of spermatogonial cells IV) CT-irradiated group showing marked degeneration, necrosis of spermatogonial cells lining seminiferous tubules and exfoliation of germ cells, V) 5 GHz + CT irradiated group reveals moderate STE loss and interstitial edema. Photomicrographs at 800× magnification (scale bar: 41 μm), using H&E staining (Green arrow: spermatids, Yellow arrow: myoid cells).

BONE MARROW CYTOLOGY

Abundant normochromatic erythrocytes (NCE-arrow) and sparse polychromatic erythrocytes (PCE) were seen in control and sham groups (**Figure 7**). The 5 GHz group shows increased PCE (green arrow) and numerous micronucleated cells (red arrow). The CT-irradiation group reveals abundant polychromatic and micronucleated cells count. Moderate NCE (green arrow) and micronucleated cells (red arrow) is seen in 5 GHz + CT group.

Fig. '7'. MayGrunwald & Giemsa staining of excised bone marrow cells from I) Negative

control group showing moderate normochromatic II) Sham irradiated group showing relatively normal arrangements of normochromatic and polychromatic erythrocytes III) 5 GHz irradiated group showing abnormally increased polychromatic and micronucleated polychromatic erythrocytes count, IV) CT-irradiated group showing high polychromatic and micronucleated erythrocytes and V) 5 GHz + CT showing moderate polychromatic and normochromatic erythrocytes count.

Discussion

Ultimately, we found gross impairments of memory, cognition, platelets, granulocyte, white blood cell and lymphocyte counts, and *p53* gene exons 5–7 banding AGE patterns in the single ionizing and non-ionizing groups, hepatocytes degeneration and reduced Leydig cells count. Intact working memory in rats can be assessed using measures of spatial working memory, through their exploratory activity in the three arms of the Y-maze. Hence, the reduced percentage alternation and number of entries in the single and combined irradiation groups in this study indicates impairment of rats' working memory with the gross impact on the CT-irradiated rats. There have been reports of a significant irradiation effect

on rats' locomotor activities where irradiation at 20 Gy resulted in a transient impairment of the cognitive functions at 7 and 20 days [19]. Elevated platelet counts in the CT- and 5 G+CT-irradiated rats, with reduced white blood cell counts in the same and 5 GHz group confirms platelets' dysregulating effects of ionizing radiation. This is consistent with Torres Filho et al.'s [20] findings of abnormally elevated platelet levels following a three-day 0–75 Gy X-irradiation in rats. However, the abnormally low platelet levels observed in the non-ionizing radiation group (5 GHz) could be a result of platelet production defects induced by auto-antibodies generation under conditions of stress as described by Semple et al. [21]. A significant reduction in lymphocyte count in the CT group indicates alterations in lymphocyte viability due to ionizing radiation exposure, which is in line with Sanzari et al.'s findings (2011) of acute lymphocyte dysfunction and compromised immune response as a function of ionizing radiation exposure coupled with hypogravity in mice at a dose rate of 0.45 Gy/min. Our study revealed 'gene deletion' effects of exon 5–7 in the *p53* gene following 14-day 5 G irradiation of rats. Additionally, the necrotized/degraded *p53* (exon 7) expression in the CT and 5G+CT groups suggests deleterious gene-

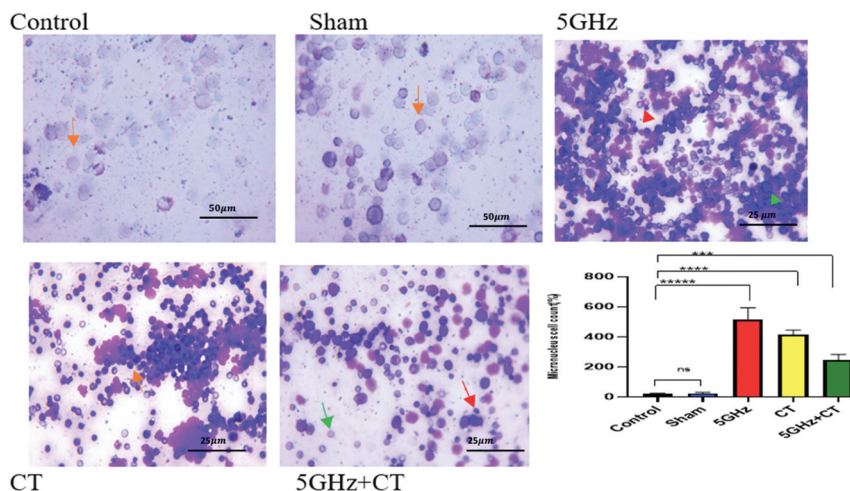


Figure 7. Photomicrographs at 100× magnification, using MayGrunwald & Giemsa staining, showing erythrocytes, polychromatic and micronucleated cells.

damaging effects of these radiations over extended periods. The significance of these findings is underscored by the role of p53 as a master regulator of cellular response to stress and its implication in genomic instability and cancer risk. Similar genotoxic effects have been validated in prenatal low-dose radiation studies [22]. The tumor suppressor p53 is a master regulator of cellular response to stress, and the activation of its transcriptional targets are both responsible for the diversity of radiation response *in vivo*. Hence, radiation-induced genomic instability such as this can predispose cells to dysregulated proliferation and maturation promoting events leading to cancer. Histological alteration of the liver cells (hepatocytes) and testicular architecture following exposure to ionizing and non-ionizing sources, especially in the CT-irradiated rats align with the association between radiation and liver damage reported in other in-vivo systems [23]. The gross degeneration of seminiferous tubules epithelium, loss of sperm, and Leydig cells in irradiated rats, especially the CT group, suggests the induction of p53 and its role in promoting deleterious nuclear transcriptional factors. This disruption of normal processes associated with spermatogenesis is consistent with findings by Nazıroğlu et al. [24] on radiation-induced damaging effects on sperm cells. A linear relationship was established between radiation exposure and aberrant, increased micronucleated erythrocyte count in our study, indicating genotoxic damage and chromosomal aberrations in irradiated rat profiles. This observation aligns with research by Bhageri et al. [25] and Smith-Roe et al. [26] on increased micronucleus formation in rats exposed to radiation.

Conclusion

We conducted one of the initial comprehensive investigations into the combined and individual effects of ionizing and non-ionizing radiation on rats exposed to 5 GHz MIMO waves before CT-irradiation. The individual radiation exposures resulted in various effects, such as increased platelet and granulocyte levels, memory and cognition

impairments, p53 gene deletions, degenerated hepatocytes, and reduced Leydig cell counts. Additionally, when high doses of ionizing radiation were combined with 5 GHz waves, mutant cells were specifically targeted for cell death. Therefore, it is crucial to consider the setup and calibration of research environments in electromagnetic field (EMF) studies, encompassing factors like specific light spectrum, flicker rates, location, placement, and calibration of wireless transmitters. Neglecting permissible limits on EMF radiation dosimetry could result in even a slight increase in the incidence of hazard zones or diseases stemming from EMF radiation exposure, carrying far-reaching consequences for public health, societal costs, and the economy.

Acknowledgments

The authors would like to thank the technical officers at the Biotechnology Centre, Afe Babalola University and Molecular Tissue Typing Laboratory, Obafemi Awolowo University Teaching Hospital for their support.


Disclosure statement

No potential conflict of interest was reported by the author(s).

Funding

The authors declare that no funds, grants, or other support were received during the preparation of this manuscript.

ORCID


Adejoke Olukayode Obajuluwa  <http://orcid.org/0000-0003-0801-205X>

James C. Lech  <http://orcid.org/0000-0001-9919-0120>

Chidiogo Chukwunweike Onwuka  <http://orcid.org/0000-0002-5654-4002>

Rahman Ayodele Bolarinwa  <http://orcid.org/0000-0003-2782-7190>

Tiwalola Madoc Obajuluwa  <http://orcid.org/0000-0002-2494-2129>

Adedamola Adediran Fafure  <http://orcid.org/0000-0002-6335-8793>

Tjaart P.J. Krüger  <http://orcid.org/0000-0002-0801-6512>

Data availability statement

All data generated or analyzed during this study are included in this published article.

Ethics declaration

The experiments were in accordance with NIH guidelines for the care and use of laboratory animals and the study was approved by the animal ethics committee of Afe Babalola University, Ado-Ekiti, Nigeria with ethical clearance issue certificate number- ABU/COS23/101.

References

- [1] Georgiou CD, Kalaitzopoulou E, Skipitari M, et al. Physical differences between man-made and cosmic microwave electromagnetic radiation and their exposure limits, and radiofrequencies as generators of biotoxic free radicals. *Radiation*. 2022;2(4):285–302. doi: [10.3390/radiation2040022](https://doi.org/10.3390/radiation2040022)
- [2] Havas M, Marrongelle J. Replication of heart rate variability provocation study with 2.4-GHz cordless phone confirms original findings. *Electromagn Biol Med*. 2013;32(2):253–266. doi: [10.3109/15368378.2013.776437](https://doi.org/10.3109/15368378.2013.776437)
- [3] Lech J, Krüger T, Boros L, et al. World Health Organization - International EMF Project - International Advisory Committee (IAC) - 11th anniversary of the International Optical radiation and 26th anniversary of EMF Project meeting. South Africa National Report 2022.
- [4] Choi K, Ha J, Bae S, et al. Mobile phone use and time trend of brain cancer incidence rate in Korea. *Bioelectromagnetics*. 2021;42(8):629–648. doi: [10.1002/bem.22373](https://doi.org/10.1002/bem.22373)
- [5] Lin Y, Gao P, Guo Y, et al. Effects of long-term exposure to L-Band high-power microwave on the brain function of male mice. *Biomed Res Int*. 2021;2021:1–9. doi: [10.1155/2021/2237370](https://doi.org/10.1155/2021/2237370)
- [6] Maluin SM, Osman K, Jaffar F, et al. Effect of radiation emitted by wireless devices on male reproductive hormones: a systematic review. *Front Physiol*. 2021;12:732420. doi: [10.3389/fphys.2021.732420](https://doi.org/10.3389/fphys.2021.732420)
- [7] Liu Q, Si T, Xu X, et al. Electromagnetic radiation at 900 MHz induces sperm apoptosis through bcl-2, bax and caspase-3 signaling pathways in rats. *Reprod Health*. 2015;12(1):65. doi: [10.1186/s12978-015-0062-3](https://doi.org/10.1186/s12978-015-0062-3)
- [8] Mahdavi SM, Sahraei H, Yaghmaei P, et al. Effects of electromagnetic radiation exposure on stress-related behaviors and stress hormones in male Wistar rats. *Biomol Ther*. 2014 Nov;22(6):570–576. Epub 2014 Nov 30. PMID: 25489427; PMCID: PMC4256039. doi: [10.4062/biomolther.2014.054](https://doi.org/10.4062/biomolther.2014.054)
- [9] Afolabi OB, Olukayode OA, Obajuluwa T, et al. Exposure to a 2.5 GHz non-ionizing electromagnetic field alters hematological profiles, biochemical parameters, and induces oxidative stress in male albino rats. *Biomed Environ Sci*. 2019;32(11):860–863. doi: [10.3967/bes2019.107](https://doi.org/10.3967/bes2019.107)
- [10] Ibitayo AO, Afolabi OB, Akinyemi AJ, et al. RAPD profiling, DNA fragmentation, and histomorphometric examination in brains of Wistar rats exposed to indoor 2.5 GHz wi-fi devices radiation. *BioMed Research International*. 2017;2017:1–6. doi: [10.1155/2017/8653286](https://doi.org/10.1155/2017/8653286)
- [11] Narayanan SN, Jetty R, Kesari KK, et al. Radiofrequency electromagnetic radiation-induced behavioral changes and their possible basis. *Environ Sci Pollut Res*. 2019;26(30):30693–30710. doi: [10.1007/s11356-019-06278-5](https://doi.org/10.1007/s11356-019-06278-5)
- [12] Obajuluwa AO, Akinyemi AJ, Afolabi OB, et al. Ishola AO. Exposure to radio-frequency electromagnetic waves alters acetylcholinesterase gene expression, exploratory and motor coordination-linked behaviour in male rats. *Toxicol Rep*. 2017;4:530–534. doi: [10.1016/j.toxrep.2017.09.007](https://doi.org/10.1016/j.toxrep.2017.09.007)
- [13] Ross CL, Siriwardane M, Almeida-Porada G, et al. The effect of low-frequency electromagnetic field on human bone marrow stem/progenitor cell differentiation. *Stem Cell Res*. 2015;15(1):96–108. doi: [10.1016/j.scr.2015.04.009](https://doi.org/10.1016/j.scr.2015.04.009)
- [14] Song K, Im SH, Yoon YJ, et al. A 60 hz uniform electromagnetic field promotes human cell proliferation by decreasing intracellular reactive oxygen species levels. *PLOS ONE* 13. 2018;13(7):e0199753. doi: [10.1371/journal.pone.0199753](https://doi.org/10.1371/journal.pone.0199753)
- [15] Green DR, Kroemer G. Cytoplasmic functions of the tumour suppressor p53. *Nature*. 2009;458(7242):1127–1130. doi: [10.1038/nature07986](https://doi.org/10.1038/nature07986)

- [16] Coskun P, Wyrembak J, Schriener SE, et al. A mitochondrial etiology of Alzheimer and Parkinson disease. *Biochim Biophys Acta Gen Subj.* 2012;1820(5):553–564. doi: [10.1016/j.bbagen.2011.08.008](https://doi.org/10.1016/j.bbagen.2011.08.008)
- [17] Wang K, Klionsky DJ. Mitochondria removal by autophagy. *Autophagy* 7. 2011;7(3):297–300. doi: [10.4161/auto.7.3.14502](https://doi.org/10.4161/auto.7.3.14502)
- [18] Lueptow LM. Novel object recognition test for the investigation of learning and memory in mice. *J Vis Exp.* 2017;126:55718. doi: [10.3791/55718-v](https://doi.org/10.3791/55718-v)
- [19] Liu Y, Xiao S, Liu J, et al. An Experimental Study of Acute Radiation-Induced Cognitive Dysfunction in a Young Rat Model. *Am J Neuroradiol.* 2010;31(2):383–387. doi: [10.3174/ajnr.A1801](https://doi.org/10.3174/ajnr.A1801)
- [20] Torres Filho IP, Torres LN, Barraza D, et al. Cellular and Biochemical effects of combined X-Ray radiation and storage on whole blood. Dose-Response. 2022;20(1):155932582110731. doi: [10.1177/15593258211073100](https://doi.org/10.1177/15593258211073100)
- [21] Semple JW, Milev Y, Cosgrave D, et al. Differences in serum cytokine levels in acute and chronic autoimmune thrombocytopenic purpura: relationship to platelet phenotype and antiplatelet T-cell reactivity. *Blood.* 1996;87(10):4245–4254. doi: [10.1182/blood.V87.10.4245.bloodjournal87104245](https://doi.org/10.1182/blood.V87.10.4245.bloodjournal87104245)
- [22] Bolaris S, Bozas E, Benekou A, et al. *In utero* radiation-induced apoptosis and p53 gene expression in the developing rat brain. *Int J Radiat Biol.* 2009;77(1):71–81. doi: [10.1080/095530001453131](https://doi.org/10.1080/095530001453131)
- [23] Fahmy H, Mohammed F. Hepatic injury induced by radio frequency waves emitted from conventional Wi-Fi devices in Wistar rats. *Hum Exp Toxicol.* 2021;40(1):136–147. doi: [10.1177/0960327120946470](https://doi.org/10.1177/0960327120946470)
- [24] Nazıroğlu M, Yüksel M, Köse SA, et al. Recent reports of wi-fi and mobile phone-induced radiation on oxidative stress and reproductive signaling pathways in females and males. *J Membr Biol.* 2013 Dec;246(12):869–875. doi: [10.1007/s00232-013-9597-9](https://doi.org/10.1007/s00232-013-9597-9)
- [25] Bhageri H, Rezapoor S, Najafi M, et al. Protection against radiation induced micronuclei in rat bone marrow erythrocytes by curcumin and selenium L-Methionine. *Iran J Med Sci.* 2018 Nov;43(6):645–652. doi: [10.1016/j.radonc.2014.06.002](https://doi.org/10.1016/j.radonc.2014.06.002)
- [26] Smith-Roe SL, Wyde ME, Stout MD, et al. Evaluation of the genotoxicity of cell phone radiofrequency radiation in male and female rats and mice following subchronic exposure. *Environ And Mol Mutagen.* 2020 Feb;61(2):276–290. doi: [10.1002/em.22343](https://doi.org/10.1002/em.22343)